




Coulomb drag of viscous electron fluids: Drag viscosity and negative drag conductivityEddwi H. Hasdeo ^{1,2}, Edvin G. Idrisov ^{1,3} and Thomas L. Schmidt ^{1,4}¹*Department of Physics and Material Science, University of Luxembourg, L-1511 Luxembourg, Luxembourg*²*Research Center for Quantum Physics, National Research and Innovation Agency, 15314 South Tangerang, Indonesia*³*Abrikosov Center for Theoretical Physics, MIPT, 141701 Institutskii per., Dolgoprudnyi, Russia*⁴*School of Chemical and Physical Sciences, Victoria University of Wellington, P.O. Box 600, Wellington 6140, New Zealand*

(Received 12 July 2022; revised 14 November 2022; accepted 1 March 2023; published 20 March 2023)

We show that Coulomb drag in bilayer systems in the regime of electron hydrodynamics leads to additional viscosity terms in the hydrodynamic equations, the drag, and drag-Hall viscosities, besides the well-known kinematic and Hall viscosities. These additional viscosity terms arise from a change of the stress tensor due to the interlayer Coulomb interactions. All four viscosity terms are tunable by varying the applied magnetic field and the electron densities in the two layers. At certain ratios between the electron densities in the two layers, the drag viscosity dramatically changes the longitudinal transport resulting in a negative drag conductivity.

DOI: [10.1103/PhysRevB.107.L121107](https://doi.org/10.1103/PhysRevB.107.L121107)

Introduction. Several decades ago, Gurzhi imagined an ideal metal from which all impurities and scatterers (e.g., phonons) were removed and which contained only electrons interacting among themselves [1]. In this case, the electrons behave collectively like a viscous fluid with a resistivity determined by their viscosity, which is inversely proportional to temperature [2]. This result differs starkly from that in a normal metal whose resistivity increases with temperature due to electron-phonon interactions. Such hydrodynamic electron flows have been realized in clean samples of GaAs [3] and more recently in graphene [4–6], PdCoO₂ [7], and in Weyl semimetals [8].

The viscous hydrodynamic regime can give rise to many surprising transport phenomena in graphene such as, for instance, an increase of the thermal conductivity and a breakdown of the Wiedemann-Franz law [4], an increase of the electrical conductance of a constriction due to superballistic viscous flow [9,10], or a nonlocal negative resistance [6]. In topological materials, quantum geometry can also lead to a peculiar electron flow [11,12]. As the viscosity plays a central role in the transport of electrons in the hydrodynamic regime, it is natural to ask how we can manipulate the viscosity experimentally. It is well-known that to a certain extent, the viscosity can be controlled by varying the temperature, the carrier density, and the impurity concentration [13,14]. On the other hand, applying a magnetic field not only modifies the viscosity but also introduces an additional *Hall* viscosity in the hydrodynamic equations [13,15–17].

If one places two layered metals parallel to each other and applies a current in one (the active) layer, the interlayer Coulomb interaction will induce a drag voltage in the other (the passive) layer [18,19]. If we consider the two metals in such a Coulomb drag setup as viscous electron fluids, we can ask if the viscosities of the two metals are modified due to the interlayer Coulomb interaction [20]. Furthermore, one could expect that the hydrodynamic equations might be modified because additional viscosity terms emerge from the

interlayer Coulomb interaction similar to the case of Hall viscosity.

In this paper, we show that two viscosity terms emerge indeed in the magneto-transport of viscous fluids in a Coulomb drag setup. For this purpose, we solve the coupled kinetic equations for the electrons in the two layers that interact via Coulomb interactions. The angular harmonics of the nonequilibrium distribution function give access to macroscopic quantities, including the stress tensor in the linear-response and low-temperature limit (with Fermi energy $E_F \gg T$). The effects of intra- and interlayer Coulomb interactions on the stress tensor lead to the conventional viscosity and the drag viscosity, respectively, in the Navier-Stokes equations (NSEs). In the presence of a magnetic field, these intra- and interlayer interactions will additionally induce the Hall and the drag-Hall viscosities.

We show that the resulting four viscosities are tunable by varying the ratio of the electron densities in the two layers and the magnetic field strength. Equipped with these four viscosities, we apply the NSE to Coulomb drag in a Hall bar geometry, where the boundary conditions lead to Poiseuille flow. Such flow has been observed in many experiments, including graphene and Weyl semimetals [21,22]. We show that in a certain range of density ratios, the drag viscosity balances the stress force from the kinematic viscosity in the passive layer and becomes stronger than the drag force. This situation causes the electrons in the passive layer to flow opposite to the flow in the active layer, a phenomenon which gives rise to a negative drag conductivity (see Fig. 1). Under an applied magnetic field, the transverse electric field shows a sign change due to the drag-Hall viscosity and is tunable by varying the density ratio.

Previous works have found negative drag conductivities in different coupled systems such as 2D-3D systems [23], 1D-1D nanowires [24], and 2D-2D systems [25]. The negative drag in the present work has a different origin from the negative drag in nanowires reported in Ref. [24] because the latter requires a low density and a high magnetic field. In contrast,

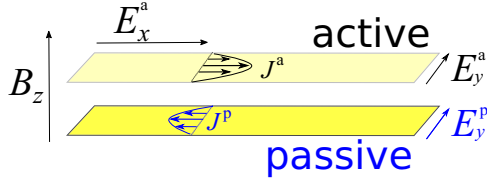


FIG. 1. Coulomb drag setup: An electric field $E_x^a \hat{x}$ is applied to the active layer causing a Poiseuille current profile $J^a(y) \hat{x}$. This current induces electron motion in the passive layer controlled by the drag coefficient γ_d^p and the drag viscosity ν_d^p . When the electron density of the passive layer is much higher than that of the active layer, γ_d^p becomes very small and J^p changes signs. The magnetic field $B_z \hat{z}$ and horizontal flow $J^p(y) \hat{x}$ cause a charge buildup and a transversal electric field $E_y^p \hat{y}$ that can be used to probe the drag-Hall viscosity ν_{dH}^p .

the negative drag presented in this work occurs at high density $E_F > T$ and does not require magnetic field. We argue that the negative drag in double bilayer graphene found in Ref. [25] might be explained by our results because it was observed at intermediate temperatures ($T \approx 100$ K) and at Fermi energies $E_F \gg k_B T$ where viscous hydrodynamic flow and momentum drag are expected.

Viscosities due to Coulomb drag. The system we consider consists of a pair of two-dimensional metallic layers separated by a distance much shorter than the screening length. To ensure hydrodynamic electron flow, we assume that the metals are clean such that the intra- and interlayer Coulomb scattering rates are much faster than those due to electron-impurity and electron-phonon scattering. Moreover, we consider an in-plane applied electric field in the active layer and allow for an applied out-of-plane magnetic field $\mathbf{B} = B_z \hat{z}$ (see Fig. 1). The macroscopic dynamics of hydrodynamic electrons at small flow velocity can then be described by the linearized NSE, derived in the Supplemental Material (SM) [26],

$$\partial_t \mathbf{u}^\lambda = \frac{e}{\alpha m} \mathcal{E}^\lambda + \omega_c \mathbf{u}^\lambda \times \hat{z} - \gamma_d^\lambda (\mathbf{u}^\lambda - \mathbf{u}^{\bar{\lambda}}) + f_{\text{visc}}^\lambda, \quad (1)$$

$$f_{\text{visc}}^\lambda = \nu^\lambda \nabla^2 \mathbf{u}^\lambda + \nu_H^\lambda \nabla^2 (\mathbf{u}^\lambda \times \hat{z}) + \nu_d^\lambda \nabla^2 \mathbf{u}^{\bar{\lambda}} + \nu_{dH}^\lambda \nabla^2 (\mathbf{u}^{\bar{\lambda}} \times \hat{z}), \quad (2)$$

where $\mathbf{u}^\lambda(\mathbf{r}, t)$ is the drift velocity of electrons in the active and passive layers, $\lambda \in \{a, p\}$ (where we use $\bar{\lambda}$ to designate the opposite layer), γ_d^λ is the rate of interlayer scattering and known as the drag coefficient and e and m are electron charge and band mass, respectively. As shown in the SM [26], the equation is also valid for Dirac electrons, in which case $m = p_F/v_F$ corresponds to the effective cyclotron mass. The band parameter $\alpha = 1$ for a parabolic band and $\alpha = 2$ for a linear band. Moreover, ν^λ is the kinematic viscosity, which is inversely proportional to the rate of intralayer scattering γ_{ee}^λ , ν_H^λ is the Hall viscosity which is proportional to the cyclotron frequency $\omega_c = eB_z/mc$, c being the speed of light. $\nu_d^\lambda \propto \gamma_d^\lambda$ is the drag viscosity, and $\nu_{dH}^\lambda \propto \omega_c \gamma_d^\lambda$ is the drag-Hall viscosity. The total electric field in a given layer is denoted by $\mathcal{E}^\lambda = \mathbf{E}^\lambda + \frac{\alpha m}{e} \nabla P^\lambda = -\nabla \varphi^\lambda$, where \mathbf{E}^λ is the externally applied

electric field and ∇P^λ is the gradient of pressure. The presence of the drag viscosity ν_d^λ and the drag-Hall viscosity ν_{dH}^λ in the NSE is one of main results in this work. In Eq. (1), we have neglected momentum relaxing (MR) scattering due to phonons or impurities. However, we show in the SM that allowing for weak MR scattering will not change the results qualitatively as long as the system remains in the hydrodynamic regime [26].

The electron-electron interaction rate in a 2D electron gas is related to the density as $\gamma_{ee}^\lambda \propto T^2/E_F^\lambda \propto 1/\bar{n}_\lambda$, where \bar{n}_λ is the carrier density. The drag coefficient γ_d^λ are tunable by varying interlayer spacing and density [27–30]. Furthermore, as we show in the SM [26], all four viscosities ν^λ , ν_d^λ , ν_H^λ , ν_{dH}^λ are adjustable by varying the density ratio $r = \bar{n}_a/\bar{n}_p$, the ratio $\Gamma_d = \gamma_d^a/\gamma_{ee}^a$, and the strength of the magnetic field $\tilde{\omega}_c = \omega_c/\gamma_{ee}^a$ as follows:

$$\begin{aligned} \nu^a &= \frac{\nu_0}{g} (1 + \Gamma_d) (r^2 (1 + 2\Gamma_d) + (2\tilde{\omega}_c)^2), \\ \nu^p &= \frac{\nu_0}{rg} r (1 + \Gamma_d) (1 + 2\Gamma_d + (2\tilde{\omega}_c)^2), \\ \nu_d^a &= r \nu_d^p = \frac{\nu_0}{rg} \sqrt{r} \Gamma_d (r (1 + 2\Gamma_d) - (2\tilde{\omega}_c)^2), \\ \nu_H^a &= \frac{\nu_0}{g} 2\tilde{\omega}_c (r \Gamma_d^2 + r^2 (1 + \Gamma_d)^2 + (2\tilde{\omega}_c)^2), \\ \nu_H^p &= \frac{\nu_0}{rg} 2\tilde{\omega}_c (r \Gamma_d^2 + (1 + \Gamma_d)^2 + (2\tilde{\omega}_c)^2), \\ \nu_{dH}^a &= r \nu_{dH}^p = \frac{\nu_0}{rg} 2\tilde{\omega}_c \sqrt{r} \Gamma_d (1 + r) (1 + \Gamma_d), \end{aligned} \quad (3)$$

where $g = r^2 (1 + 2\Gamma_d)^2 + [2r\Gamma_d^2 + (1 + r^2)(1 + \Gamma_d)^2] (2\tilde{\omega}_c)^2 + (2\tilde{\omega}_c)^4$ and $\nu_0 = (v_F^a)^2/(4\gamma_{ee}^a)$ is the kinematic viscosity at vanishing magnetic field and drag coefficient [13,31]. We simplify the notation by measuring passive layer properties with respect to those of the active layer, $\gamma_{ee,d}^a = \gamma_{ee,d} = \gamma_{ee,d}^p/r$ and $v_F^a = v_F = \sqrt{r} v_F^p$. In the limits of $\tilde{\omega}_c \ll 1$, ν^λ and ν_d^λ take simple forms $\nu^a = r^2 \nu^p = \nu [1 - O(\tilde{\omega}_c^2)]$, where $\nu = \nu_0 (1 + \Gamma_d)/(1 + 2\Gamma_d)$ and $\nu_d^a = r \nu_d^p = \nu_d / (r^{3/2}) [1 - O(\tilde{\omega}_c^2)]$, where $\nu_d = \nu_0 \Gamma_d / (1 + 2\Gamma_d)$. In the same limits, ν_H^λ and ν_{dH}^λ are proportional to $\tilde{\omega}_c [1 - O(\tilde{\omega}_c^2)]$.

In Fig. 2(a), we show the kinematic viscosity of the active layer as a function of the magnetic field. The dashed line refers to the limit of vanishing drag coefficient $\gamma_d = 0$ whereas the solid lines with different colors correspond to different density ratios $r = \bar{n}_a/\bar{n}_p$ and fixed $\Gamma_d = 0.5$. We normalize all viscosities with respect to ν_0 . In the presence of drag, the viscosity decreases similarly to the case of MR scattering. Changing the density in the passive layer does not change significantly the viscosity in the active layer as shown by the behavior of ν^a versus r . At large magnetic fields, the viscosity decreases following the trend $1 - O(\tilde{\omega}_c^2)$, leading to a negative magnetoresistance $\propto B_z^2$ in the viscous fluid [15]. The viscosity of the passive layer in Fig. 2(e) shows a similar ω_c dependence as ν^a but is proportional to r^{-2} , implying the shown density dependence of the viscosity. The drag viscosities ν_d^λ in Figs. 2(b) and 2(f) vanish at zero drag $\gamma_d = 0$ and strongly depend on density ratio r with different dependencies

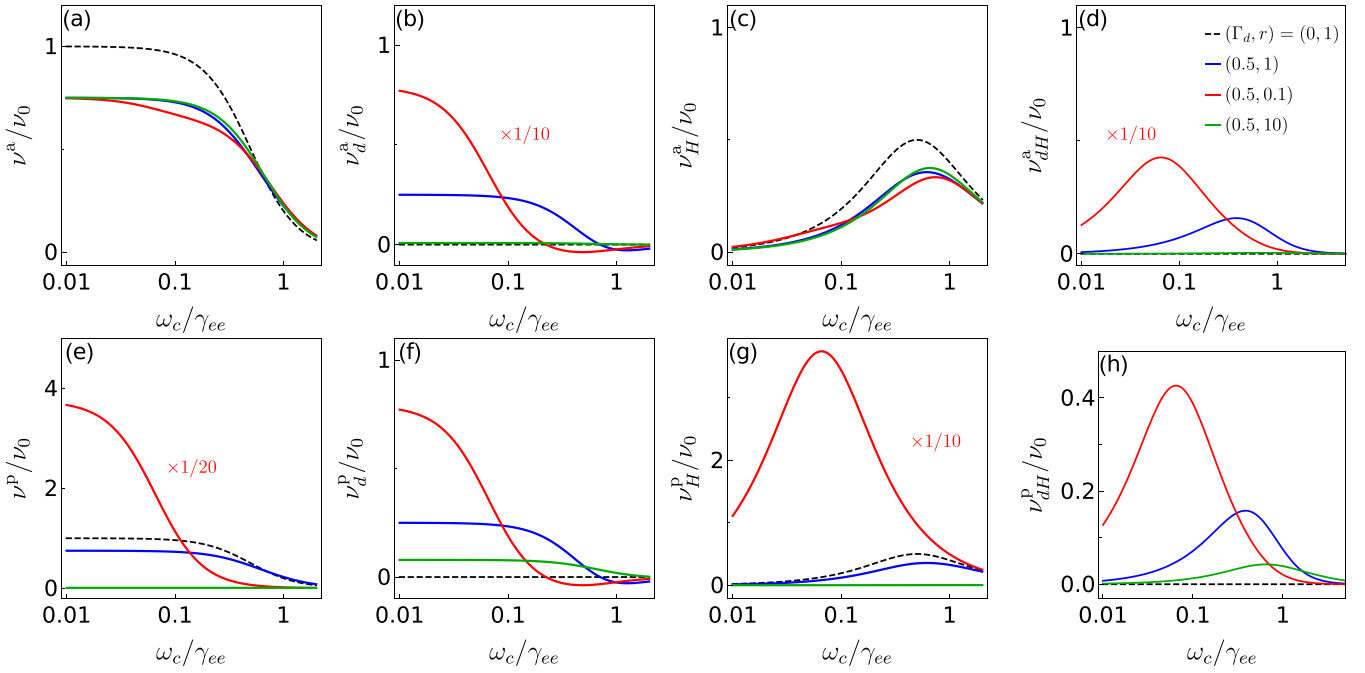


FIG. 2. The viscosities in both layers. (a), (e) The kinematic viscosity ν^λ ; (b), (f) the drag viscosity ν_d^λ ; (c), (g) the Hall viscosity ν_H^λ ; and (d), (h) the drag-Hall viscosity ν_{dH}^a in the active and passive layers, respectively, for different magnetic fields, drag coefficients $\Gamma_d = \gamma_d/\gamma_{ee}$, and density ratios $r = \bar{n}_a/\bar{n}_p$. In (b), (c), (e), and (g), we have multiplied the red lines ($\Gamma_d = 0.5$ and $r = 0.1$) by the factors written in the plot. Here $\nu_0 = (v_F^a)^2/(4\gamma_{ee}^a)$.

in active and passive layers. ν_d^λ can even become negative at large enough magnetic fields $\tilde{\omega}_c = \sqrt{r(1+2\Gamma_d)}/2$.

The Hall viscosity $\nu_H^a \propto \tilde{\omega}_c[1 - O(\tilde{\omega}_c^2)]$ shows a monotonic increase with ω_c as long as $\omega_c \ll \gamma_{ee}$. At larger ω_c , it reaches a peak and reduces to zero. ν_H^p shows a similar qualitative ω_c dependence as ν_H^a with quantitative differences in the r dependence [Fig. 2(g)]. A nonzero drag Hall viscosity ν_{dH}^λ requires both ω_c and γ_d to be simultaneously nonzero [Figs. 2(d) and 2(h)]. By changing the density ratio r , the drag-Hall viscosity ν_{dH}^a can be made larger than ν_H^a .

Effects on Poiseuille flow. Next, we specialize Eq. (1) to the case of steady-state Poiseuille flow in a narrow strip along the x direction. We apply an electric field $\mathcal{E}^a = E_x^a \hat{x}$ in the active layer and set $\mathcal{E}^p = 0$. In the presence of an applied vertical magnetic field, a transversal electric field E_y^λ builds up that ensures zero Hall current ($u_y^\lambda = 0$) at equilibrium as imposed by the boundary conditions. We obtain the following equations for the longitudinal component (see SM [26] for details):

$$\gamma_d(u^a - u^p) = \nu \partial_y^2 u^a + \frac{\nu_d}{r\sqrt{r}} \partial_y^2 u^p + \frac{e}{\alpha m} E_x^a, \quad (4)$$

$$r\gamma_d(u^p - u^a) = \frac{\nu}{r^2} \partial_y^2 u^p + \frac{\nu_d}{\sqrt{r}} \partial_y^2 u^a, \quad (5)$$

where we have made the ansatz that $\mathbf{u}^\lambda = (u^\lambda, 0)$ and assumed a fully developed flow where $u^\lambda(y)$ is independent of x . In that case, $\nabla \rightarrow \partial_y$ and we have taken $\omega_c/\gamma_{ee} \ll 1$ to simplify the r dependence of the coefficients. It is important to note that at small ω_c , the effect of the magnetic field is negligible in the longitudinal motion. For Dirac fermions with linear spectrum, one needs to replace $\sqrt{r} \rightarrow 1$, which is related to v_F^a/v_F^p , in

the denominators of Eqs. (4) and (5). Hereafter, we focus only on the case of parabolic band.

Examining the dynamics in the passive layer using Eq. (5), one finds that u^p will be parallel to u^a due to the drag force ($\propto \gamma_d$) if one disregards the ν_d term. In the presence of ν_d and at small r , however, the drag force becomes negligible in comparison to the viscosity term. As a result, it emerges from Eq. (5) that the ν_d term will enforce a balance of stress forces with the ν term, resulting in opposite curvatures of the velocity profiles u^a and u^p along the transversal direction y (see Fig. 1). In the case of no-slip boundary condition at the edges, the velocities vanish at the edges such that $u^\lambda(\pm w_h) = 0$, where $w_h = W/2$ is the half width of the system, while the velocity reaches a maximum at the center, thus creating a parabolic Poiseuille profile along y . The opposite curvatures of the velocity profiles between the two layers entail that $u^a(y)$ and $u^p(y)$ have opposite signs. One might argue that the balance of stresses arising from ν and ν_d can be diminished by inducing a pressure gradient ∇P^p or an internal electric field in the passive layer. However, this effect is weak in the limit where the flow is incompressible and kept at a constant temperature along the flow. In the following, we will see that the negative drag persists in a large window of r and even for $r = 1$.

For general values of r , the solutions of Eqs. (4) and (5) are $u^{a,p} = u_0(\tilde{u}_+ \pm \tilde{u}_-)/2$, where $u_0 = eE_x^a w_h^2/(mv)$ and

$$\tilde{u}_- = \frac{1 + r^{3/2}\tilde{\nu}_d}{\tilde{\gamma}_d(1 + r^3 + 2r^{3/2}\tilde{\nu}_d)} \left(1 - \frac{\cosh(q\tilde{y})}{\cosh(q)} \right), \quad (6)$$

$$\tilde{u}_+ = (1 - \tilde{y}^2)\xi + \left(\frac{1 - r^3}{1 + r^3 + 2r^{3/2}\tilde{\nu}_d} \right) \tilde{u}_-, \quad (7)$$

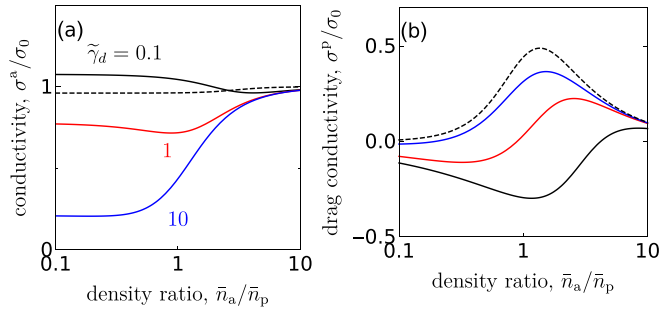


FIG. 3. (a) Conductivity σ^a and (b) drag conductivity σ^p as a function of $r = \bar{n}_a/\bar{n}_p$ for several values of $\tilde{\gamma}_d$. In this plot, we have used $v_d/v = 1/3$ and $\sigma_0 = n_a e^2 w_h^2 / (3mv)$. The dashed lines correspond to $\tilde{\gamma}_d = 0.1$ and neglect the drag viscosity.

and

$$\tilde{q} = \left(\frac{\tilde{\gamma}_d(1+r^3+2r^{3/2}\tilde{v}_d)}{1-\tilde{v}_d^2} \right)^{1/2},$$

$$\xi = \frac{r^3}{1+r^3+2r^{3/2}\tilde{v}_d}. \quad (8)$$

Here, we used the dimensionless parameters $\tilde{y} = y/w_h$, $\tilde{v}_d = v_d/v$, and $\tilde{\gamma}_d = \gamma_d w_h^2 / v = \Gamma_d W^2 / (l_{ee}^2 \tilde{v})$, where $l_{ee} = v_F / \gamma_{ee}$ and $\tilde{v} = v/v_0$. Writing the averaged charge current across the transversal direction $y \in [-w_h, w_h]$ as $\langle J^\lambda \rangle = \bar{n}_\lambda e \langle u^\lambda \rangle$, where $\langle O \rangle = \frac{1}{2} \int_{-1}^1 d\tilde{y} O$ and defining the normal and the drag conductivities as $\sigma^\lambda = \langle J^\lambda \rangle / E_x^a$, we obtain

$$\sigma^a = \frac{\bar{n}_a e^2 w_h^2}{mv} \left[\frac{1}{3} \xi + \langle \tilde{u}_- \rangle \left(\frac{1+r^3+2r^{3/2}\tilde{v}_d}{1+r^3+2r^{3/2}\tilde{v}_d} \right) \right], \quad (9)$$

$$\sigma^p = \frac{\bar{n}_p e^2 w_h^2}{mv} \left[\frac{1}{3} \xi - \langle \tilde{u}_- \rangle \left(\frac{r^3+r^{3/2}\tilde{v}_d}{1+r^3+2r^{3/2}\tilde{v}_d} \right) \right]. \quad (10)$$

In Fig. 3, we plot $\sigma^{a,p}$ as a function of density ratio r for several values of $\tilde{\gamma}_d$ and a fixed parameter $\tilde{v}_d = 1/3$ corresponding to $\gamma_d/\gamma_{ee} = 0.5$. The dashed lines correspond to the case when we neglect v_d . By increasing $\tilde{\gamma}_d$, σ^a decreases, indicating the increase of the drag resistance. At small r , the drag resistance from the other layer is very strong, leading to small values of σ^a . In the nonviscous regime $\tilde{\gamma}_d \gg 1$ (the blue line), we can see a monotonic increase of σ^a as function of r which saturates at $\sigma_0 = n_a e^2 w_h^2 / (3mv)$ for large r where the effect of the drag force is minimal. The scale factor σ_0 is the conductivity of the viscous fluid without the drag effect, which takes the shape of a Drude conductivity where the effective lifetime depends on the channel width and the viscosity $\tau_v = w_h^2 / (3v)$. In the highly viscous regime, $\tilde{\gamma}_d \ll 1$ (black line), the drag viscosity can enhance the conductivity at small r originating from the second term of Eq. (9), see the dashed line when $v_d = 0$.

The impact of v_d is most pronounced for the drag conductivity σ^p , see Fig. 3(b). At small density ratio r and in the viscous regime $\tilde{\gamma}_d < 1$, σ^p becomes negative signifying a counterflow in the passive layer with respect to the active one. At $r = 0$, σ^p becomes zero because the drag coefficient $r\gamma_d$ vanishes, and it vanishes as well at very large r because

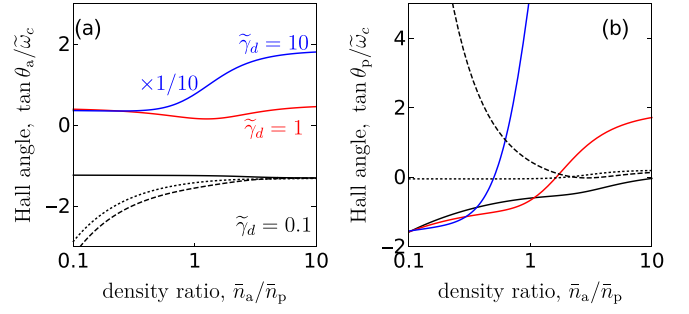


FIG. 4. (a) Hall angles at the first layer $\tan \theta_a / \tilde{\omega}_c$ and (b) at the second layer $\tan \theta_p / \tilde{\omega}_c$ as a function of $r = \bar{n}_a/\bar{n}_p$ for several values of $\tilde{\gamma}_d = \Gamma_d \mathcal{R}$. Here $\tilde{\omega}_c = \omega_c / \gamma_{ee}$ and $\Gamma_d = 0.5$. The dashed lines are for $\tilde{\gamma}_d = 0.1$ and neglecting the drag-Hall viscosity $v_{dH} = 0$ and the dotted lines are for $\tilde{\gamma}_d = 0.1$ and $v_{dH} = 0$ and $v_d = 0$.

$n_p \rightarrow 0$, see Eq. (10). A negative σ^p occurs in the viscous regime when the effect of the γ_d term is smaller than those of the v and v_d terms, see Eq. (5), causing opposite signs of u^a and u^p due to the stress balance. Indeed, when we set $v_d = 0$, σ^p never reaches a negative value (dashed line). Overall, the value of $|\sigma^p|$ is typically smaller than that of σ^a but at large $\tilde{\gamma}_d$, σ^p/σ^a can approach unity at $r = 1$.

We note that the ratio of length scales W/l_{ee} as well as Γ_d become key to observing the negative drag conductivity. The strongly interacting regime at low densities should be avoided because it entails a large value of $\tilde{\gamma}_d$ which will hamper the negative drag. It is thus preferable to be near the Fermi liquid regime with $W/l_{ee} \approx 1$. Γ_d has been estimated in the SM to be around 0.5 for double bilayer graphene separated with a distance of 1 nm and surrounded by hexagonal boron nitride dielectrics [26]. This will yield $\tilde{\gamma}_d = 2/3$. The negative drag conductivity we found may have already been observed in double bilayer graphene in Ref. [25]. In that work, the negative drag occurs at temperatures around 100 K, which is the typical parameter regime for hydrodynamics transport. At $r = 1$, the drag resistivity was found to be negative at densities corresponding to Fermi energies $E_F \gg k_B T$.

One can also consider the transverse component in Eq. (1) to relate the velocity along the strip u^λ with the perpendicular electric field E_y^λ due to the magnetic field:

$$v_H^\lambda \partial_y^2 u^\lambda + v_{dH}^\lambda \partial_y^2 u^\lambda = \frac{e}{m} E_y^\lambda - \omega_c u^\lambda. \quad (11)$$

Since u^λ is proportional to E_x^a , one can measure the Hall angle $\tan \theta_\lambda = E_y^\lambda / E_x^a$. Utilizing Eqs. (6) and (7), we obtain $\tan \theta_\lambda$ as shown in Fig. 4. At small magnetic field $\omega_c / \gamma_{ee} = \tilde{\omega}_c \ll 1$, $\tan \theta_\lambda$ is linearly proportional to the strength of the magnetic field $\tilde{\omega}_c$. The polarity of E_y^λ is less sensitive to r but more sensitive to the change of the factor $\mathcal{R} = W^2 / (l_{ee}^2 \tilde{v})$ represented by $\tilde{\gamma}_d = \mathcal{R} \Gamma_d$ in Fig. 4. On the other hand, in the passive layer, E_y^p changes signs when changing r but is less sensitive to the change of $\tilde{\gamma}_d$. The presence or absence of v_d and v_{dH} also changes the polarity of E_y^p as shown in the dashed and dotted lines in comparison to the solid line.

Conclusion. Starting from the kinetic equation for two metallic layers interacting via the Coulomb interaction, we have shown that viscous hydrodynamic transport in such a Coulomb drag setup is characterized by four viscosities: the

kinematic, Hall, drag, and drag-Hall viscosities. Those viscosities are tunable by varying parameters such as the applied magnetic field, the charge density ratio in the layers, and the drag coefficient (interlayer spacing). We showed that the drag viscosity can lead to a counterflow between electrons in the passive layer and the active one in the viscous regime. This phenomenon can be measured via a negative drag conductivity σ^P and is independent of the magnetic field in the small-field regime $\omega_c \ll \gamma_{ee}$. In the presence of a magnetic

field, the polarity of the Hall fields E_y^λ can be altered by varying the density ratio to probe the presence of the drag-Hall viscosity.

Acknowledgments. The authors acknowledge a fruitful discussion with M. Hamzah Fauzi. The authors acknowledge support from the National Research Fund Luxembourg under Grants No. CORE C20/MS/14764976/TOPREL, No. CORE C21/MS/15752388/NavSQM, and No. CORE C19/MS/13579612/HYBMES.

-
- [1] R. N. Gurzhi, Minimum of resistance in impurity-free conductors, *Zh. Eksp. Teor. Fiz.* **44**, 771 (1963) [*Sov. Phys. JETP* **17**, 521 (1963)].
- [2] A. V. Andreev, S. A. Kivelson, and B. Spivak, Hydrodynamic Description of Transport in Strongly Correlated Electron Systems, *Phys. Rev. Lett.* **106**, 256804 (2011).
- [3] M. J. M. de Jong and L. W. Molenkamp, Hydrodynamic electron flow in high-mobility wires, *Phys. Rev. B* **51**, 13389 (1995).
- [4] J. Crossno, J. K. Shi, K. Wang, X. Liu, A. Harzheim, A. Lucas, S. Sachdev, P. Kim, T. Taniguchi, K. Watanabe, T. A. Ohki, and K. C. Fong, Observation of the Dirac fluid and the breakdown of the Wiedemann-Franz law in graphene, *Science* **351**, 1058 (2016).
- [5] D. A. Bandurin, I. Torre, R. K. Kumar, M. B. Shalom, A. Tomadin, A. Principi, G. H. Auton, E. Khestanova, K. S. Novoselov, I. V. Grigorieva, L. A. Ponomarenko, A. K. Geim, and M. Polini, Negative local resistance caused by viscous electron backflow in graphene, *Science* **351**, 1055 (2016).
- [6] L. Levitov and G. Falkovich, Electron viscosity, current vortices and negative nonlocal resistance in graphene, *Nat. Phys.* **12**, 672 (2016).
- [7] P. J. W. Moll, P. Kushwaha, N. Nandi, B. Schmidt, and A. P. Mackenzie, Evidence for hydrodynamic electron flow in PdCoO₂, *Science* **351**, 1061 (2016).
- [8] J. Gooth, F. Menges, N. Kumar, V. Süß, C. Shekhar, Y. Sun, U. Drechsler, R. Zierold, C. Felser, and B. Gotsmann, Thermal and electrical signatures of a hydrodynamic electron fluid in tungsten diphosphide, *Nat. Commun.* **9**, 4093 (2018).
- [9] H. Guo, E. Ilseven, G. Falkovich, and L. S. Levitov, Higher-than-ballistic conduction of viscous electron flows, *Proc. Natl. Acad. Sci. USA* **114**, 3068 (2017).
- [10] R. Krishna Kumar, D. A. Bandurin, F. M. D. Pellegrino, Y. Cao, A. Principi, H. Guo, G. H. Auton, M. Ben Shalom, L. A. Ponomarenko, G. Falkovich, K. Watanabe, T. Taniguchi, I. V. Grigorieva, L. S. Levitov, M. Polini, and A. K. Geim, Superballistic flow of viscous electron fluid through graphene constrictions, *Nat. Phys.* **13**, 1182 (2017).
- [11] E. H. Hasdeo, J. Ekström, E. G. Idrisov, and T. L. Schmidt, Electron hydrodynamics of two-dimensional anomalous Hall materials, *Phys. Rev. B* **103**, 125106 (2021).
- [12] R. Toshio, K. Takasan, and N. Kawakami, Anomalous hydrodynamic transport in interacting noncentrosymmetric metals, *Phys. Rev. Res.* **2**, 032021(R) (2020).
- [13] F. M. D. Pellegrino, I. Torre, and M. Polini, Nonlocal transport and the Hall viscosity of two-dimensional hydrodynamic electron liquids, *Phys. Rev. B* **96**, 195401 (2017).
- [14] A. Lucas and K. C. Fong, Hydrodynamics of electrons in graphene, *J. Phys.: Condens. Matter* **30**, 053001 (2018).
- [15] P. S. Alekseev, Negative Magnetoresistance in Viscous Flow of Two-Dimensional Electrons, *Phys. Rev. Lett.* **117**, 166601 (2016).
- [16] T. Scaffidi, N. Nandi, B. Schmidt, A. P. Mackenzie, and J. E. Moore, Hydrodynamic Electron Flow and Hall Viscosity, *Phys. Rev. Lett.* **118**, 226601 (2017).
- [17] A. I. Berdyugin, S. G. Xu, F. M. D. Pellegrino, R. K. Kumar, A. Principi, I. Torre, M. B. Shalom, T. Taniguchi, K. Watanabe, I. V. Grigorieva, M. Polini, A. K. Geim, and D. A. Bandurin, Measuring Hall viscosity of graphene's electron fluid, *Science* **364**, 162 (2019).
- [18] B. N. Narozhny and A. Levchenko, Coulomb drag, *Rev. Mod. Phys.* **88**, 025003 (2016).
- [19] A.-P. Jauho and H. Smith, Coulomb drag between parallel two-dimensional electron systems, *Phys. Rev. B* **47**, 4420 (1993).
- [20] Y. Liao and V. Galitski, Drag viscosity of metals and its connection to Coulomb drag, *Phys. Rev. B* **101**, 195106 (2020).
- [21] J. A. Sulpizio, L. Ella, A. Rozen, J. Birkbeck, D. J. Perello, D. Dutta, M. Ben-Shalom, T. Taniguchi, K. Watanabe, T. Holder, R. Queiroz, A. Principi, A. Stern, T. Scaffidi, A. K. Geim, and S. Ilani, Visualizing Poiseuille flow of hydrodynamic electrons, *Nature (London)* **576**, 75 (2019).
- [22] U. Vool, A. Hamo, G. Varnavides, Y. Wang, T. X. Zhou, N. Kumar, Y. Dovzhenko, Z. Qiu, C. A. C. Garcia, A. T. Pierce, J. Gooth, P. Anikeeva, C. Felser, P. Narang, and A. Yacoby, Imaging phonon-mediated hydrodynamic flow in WTe₂, *Nat. Phys.* **17**, 1216 (2021).
- [23] P. M. Solomon, P. J. Price, D. J. Frank, and D. C. La Tulipe, New Phenomena in Coupled Transport Between 2D and 3D Electron-Gas Layers, *Phys. Rev. Lett.* **63**, 2508 (1989).
- [24] M. Yamamoto, M. Stopa, Y. Tokura, Y. Hirayama, and S. Tarucha, Negative Coulomb drag in a one-dimensional wire, *Science* **313**, 204 (2006).
- [25] J. I. A. Li, T. Taniguchi, K. Watanabe, J. Hone, A. Levchenko, and C. R. Dean, Negative Coulomb Drag in Double Bilayer Graphene, *Phys. Rev. Lett.* **117**, 046802 (2016).
- [26] See Supplemental Material at <http://link.aps.org/supplemental/10.1103/PhysRevB.107.L121107> for the detailed derivation of the four viscosities, the effect of momentum relaxing collisions

- caused by impurities or phonons, Coulomb drag scattering integral, Hall dynamics and Hall angle.
- [27] V. F. Gantmakher and I. B. Levinson, Effect of collisions between carriers on the dissipative conductivity, *Zh. Eksp. Teor. Fiz.* **74**, 261 (1978) [*Sov. Phys. JETP* **41**, 133 (1978)].
- [28] D. A. Abanin, R. V. Gorbachev, K. S. Novoselov, A. K. Geim, and L. S. Levitov, Giant Spin-Hall Effect Induced by the Zeeman Interaction in Graphene, *Phys. Rev. Lett.* **107**, 096601 (2011).
- [29] J. C. W. Song, D. A. Abanin, and L. S. Levitov, Coulomb drag mechanisms in graphene, *Nano Lett.* **13**, 3631 (2013).
- [30] D. X. Nguyen, G. Wagner, and S. H. Simon, Quantum Boltzmann equation for bilayer graphene, *Phys. Rev. B* **101**, 035117 (2020).
- [31] P. Ledwith, H. Guo, A. Shytov, and L. Levitov, Tomographic Dynamics and Scale-Dependent Viscosity in 2D Electron Systems, *Phys. Rev. Lett.* **123**, 116601 (2019).